NeuroImage xxx (2013) xxx–xxx

Contents lists available at SciVerse ScienceDirect

NeuroImage

journal homepage: www.elsevier.com/locate/ynimg

Partial least squares correlation of multivariate cognitive abilities and local brain structure in children and adolescents

G. Ziegler [a,*], R. Dahnke [a], A.D. Winkler [a], C. Gaser [a,b]

[a] Department of Psychiatry, Jena University Hospital, Jena, Germany
[b] Department of Neurology, Jena University Hospital, Jena, Germany

ARTICLE INFO

Article history:
Accepted 21 May 2013
Available online xxxx

Keywords:
Brain morphology
Development
Intelligence
Partial least squares
Multivariate analysis

ABSTRACT

Intelligent behavior is not a one-dimensional phenomenon. Individual differences in human cognitive abilities might be therefore described by a 'cognitive manifold' of intercorrelated tests from partially independent domains of general intelligence and executive functions. However, the relationship between these individual differences and brain morphology is not yet fully understood. Here we take a multivariate approach to analyzing covariations across individuals in two feature spaces: the low-dimensional space of cognitive ability subtests and the high-dimensional space of local gray matter volume obtained from voxel-based morphometry. By exploiting a partial least squares correlation framework in a large sample of 286 healthy children and adolescents, we identify directions of maximum covariance between both spaces in terms of latent variable modeling. We obtain an orthogonal set of latent variables representing commonalities in the brain–behavior system, which emphasize specific neuronal networks involved in cognitive ability differences. We further explore the early lifespan maturation of the covariance between cognitive abilities and local gray matter volume. The dominant latent variable revealed positive weights across widespread gray matter regions (in the brain domain) and the strongest weights for parents' ratings of children's executive function (in the cognitive domain). The obtained latent variables for brain and cognitive abilities exhibited moderate correlations of 0.46–0.6. Moreover, the multivariate modeling revealed indications for a heterochronic formation of the association as a process of brain maturation across different age groups.

Introduction

A major goal of human development research is to identify the functional and structural processes that are predictive of individual cognitive skills (Tau and Peterson, 2010). magnetic resonance imaging (MRI) and computational morphometry have become invaluable tools for *in-vivo* exploration of the underlying changes in healthy brain maturation (Mietchen and Gaser, 2009; Toga and Thompson, 2003). On the one hand, research focused on commonalities shared by children with typical pediatric development has revealed that the general course of brain structure development is distinct in different brain regions and tissue types (Giedd and Rapoport, 2010; Lenroot and Giedd, 2006). Studies observed inverted-U shaped and curvilinear trajectories in gray matter volume (GMV) Gogtay et al., 2004; Lenroot et al., 2007 and cortical thickness (CT) (Shaw, 2008; Shaw et al., 2006; Sowell et al., 2004), and rather continuous increases in white matter volume (WMV) into early adulthood (Ostby et al., 2009; Tamnes et al., 2010c). In addition, trajectories of brain maturation exhibited a substantial sexual dimorphism with delayed peaks in male GMV (Lenroot et al., 2007) and CT (Shaw, 2008) development. On the other hand, there is a growing interest in the individual variability of structural maturational patterns and its relation to differences in cognitive abilities and behavior during adulthood (Deary et al., 2010; Kanai and Rees, 2011). The general intelligence factor, *i.e.* the g-factor, possesses impressive predictive validity for lifespan educational and occupational success, as well as social mobility (Deary, 2012). However, the causes and neurodevelopmental mechanisms underlying individual differences of stable cognitive abilities in adults are still unresolved. Studies exploring general intelligence in relation to brain morphology have been conducted in children and adolescents (Karama et al., 2009, 2011; Lange et al., 2010; Luders et al., 2011; Shaw et al., 2006; Tamnes et al., 2011; Wilke et al., 2003) and younger and middle-aged adults (Haier et al., 2004; Luders et al., 2007, 2008, 2009b; Narr et al., 2007; Tamnes et al., 2011). In addition, recent studies have focused on more specific cognitive abilities and skills in the verbal domain (Porter et al., 2011; Ramsden et al., 2011), working memory (Østby et al., 2011, 2012), and executive functions (Tamnes et al., 2010c). A broad set of cognitive processes contributes to what is commonly referred to as executive functions. Among others, this includes planning, working memory, problem solving and inhibition of responses (Chan et al., 2008). There is neuropsychological and non-clinical evidence for a relation of executive functions to general intelligence (Ackerman et al., 2005; Ardila et al., 2000; Friedman et al., 2008; Salthouse et al., 2003;

* Corresponding author at: Center for Neuroimaging, Jahnstrasse 3, 07743 Jena, Germany.
E-mail address: Gabriel.Ziegler@uni-jena.de (G. Ziegler).

1053-8119/$ – see front matter © 2013 Published by Elsevier Inc.
http://dx.doi.org/10.1016/j.neuroimage.2013.05.088

Shelton et al., 2009), but as suggested by Friedman et al. (2006) the current intelligence measures do not sufficiently assess these executive control abilities as a contributing factor to 'intelligent behavior'. Thus, in order to capture the complexity of individual differences in cognitive abilities, tests should assess both domains of intelligence and executive function.

Partial least squares framework

Recent studies have emphasized the potential of multivariate analyses for brain development data in general (Bray et al., 2009) and brain maturation in particular (Dosenbach et al., 2010; Hoeft et al., 2011; Lerch et al., 2006; Misaki et al., 2012). The partial least squares (PLS) approach is a class of latent variable algorithms initially originated by Herman Wold (Wold, 1975, 1982) to model associations between two or more blocks of indicators of a system by means of latent variables (Geladi, 1988; Hoeskuldsson, 1988; Wegelin, 2000). PLS has proven to be particularly useful when the number of observations is much smaller than the number of indicators. In addition to applications in psychology, economics, chemometrics and medicine, PLS was successfully introduced to identify associations between multiple behavioral predictors and whole brain activity correlates derived from PET and fMRI (Koutsouleris et al., 2010; Krishnan et al., 2011; McIntosh and Lobaugh, 2004; McIntosh et al., 1996, 2004). There are several advantages of PLS for the purpose of modeling the relationship among local brain structure and multivariate cognitive abilities:

Firstly, the PLS framework naturally extends the classical latent variable approach to cognitive ability tests (Bartholomew, 2004; Carroll, 1993; Jensen, 1998; Spearman, 1904) in a way that directly includes structural properties of brains in the very process of modeling individual differences. In particular, neuroimaging studies that investigate multivariate aspects of individual differences of cognitive abilities (*e.g.* (Barbey et al., 2012; Colom et al., 2006, 2007, 2010; Ebisch et al., 2012; Gläscher et al., 2010; Karama et al., 2011)) often apply an analysis procedure with the following two *separate* steps. (A) At first a measurement model of multiple cognitive tests is used to obtain valid estimates of specific cognitive domains or to extract higher order intelligence factors. (B) Afterwards the obtained domain- or factor scores are related to the structural brain data using the general linear model in a mass-univariate manner. Using (A) and (B) basically corresponds to decomposing the unknown multivariate mapping F: $C \rightarrow B$ of the 'cognitive abilities space' to the 'brain structure space' into separate univariate mappings for each voxel/vertex and cognitive domain/factor. By applying PLS we propose a fundamentally different approach that jointly models individual differences in both multivariate spaces in a single generative model of latent variables. Instead of exploring neuronal correlates of *a-priori* fixed cognitive constructs this generalizes the covariance to a multivariate problem with free weightings in both spaces. Moreover, the major difference is that the optimal feature weighting in both spaces is driven by the maximum covariances (see *e.g.* Shawe-Taylor and Cristianini, 2004) instead of maximizing (error-free) variance in factor analysis or latent variable modeling of cognitive tests.

Secondly, the PLS approach is an exploratory method that affords the analysis of structural patterns through the entire brain. PLS overcomes the limitation of the numbers of observed variables in structural equation modeling (SEM) and thus allows the analysis of MR-based images with tens or hundreds of thousands of voxels or vertices without *a-priori* selection of certain ROIs.

Thirdly, PLS models overcome a limitation of mass-univariate approaches by increasing the sensitivity to detect subtle or spatially distributed effects in brain signals (McIntosh and Lobaugh, 2004). Unlike the general linear model (Monti, 2011, for review), PLS explicitly allows modeling effects of numerous strongly collinear or near-linear dependent indicators (Wegelin, 2000), which is especially true for cognitive ability tests (Jensen, 1998).

Fourthly, in contrast to the alternative and very similar canonical correlation analysis (CCA) (Borga et al., 1992, for a unified framework of PLS and CCA), the coefficients derived from PLS modeling were found to be easier to interpret and more stable (Wegelin, 2000). This is mainly because the coefficients in PLS models express the bivariate contribution of each indicator to the latent variables which is in contrast to the mutually dependent coefficients derived from CCA that 'behave' more like multiple linear regression coefficients.

The aim of the current study was to identify latent variables underlying multiple cognitive abilities and local brain structure in a large sample of 286 healthy children and adolescents from the NIH study of normal brain development. By using partial least squares correlation (PLSC) and voxel-based morphometry (VBM) we explored gray matter networks that covaried with a broad set of 19 abilities tests in the domains of intelligence, processing speed, and executive functioning. Finally, we explored age-related maturational differences of the covariance in age groups of younger and older children, and adolescents.

Materials and methods

Modeling cognitive abilities and local brain structure in the PLS framework

Though the PLS framework is much more general we here only focus on the two-block case and use it to jointly analyze individual differences in a set of behavioral predictors and spatial brain variables. We assume the cognitive data and the brain data is represented in two matrices (or blocks) $\mathbf{X}$ and $\mathbf{Y}$, respectively $l \times m$ and $l \times n$. The columns of $\mathbf{X}$ correspond to cognitive test data, *e.g.* total IQ scores or verbal span. The columns of $\mathbf{Y}$ contain voxelwise structural brain features after normalization and registration, in particular local gray matter volume maps obtained from VBM. In order to avoid variance differences that may bias the PLS modeling steps, we assume the columns of $\mathbf{X}$ and $\mathbf{Y}$ to be standardized features, *e.g.* z-scores. The main idea here is that individual differences observed in $\mathbf{X}$ and $\mathbf{Y}$ are generated by two latent variables, say ζ and ξ, respectively. In other words, the columns in $\mathbf{X}$ and $\mathbf{Y}$ are assumed to be indicators for the *a-priori* unknown variables ζ and ξ which we estimate from the data. Importantly, ζ and ξ are assumed to covary, in order to represent the cross-covariance of the indicators $\mathbf{X}^T\mathbf{Y}$ at the level (of error free) latent variables, which makes PLSC a special case of structural equation modeling (SEM). A graphical path model representation of the above outlined idea is depicted in Fig. 1A. Our goal to identify directions of maximum covariance in the multivariate observations $\mathbf{X}$ and $\mathbf{Y}$ can be further formalized:

$$\sigma_1 = Cov(\zeta_1, \xi_1) = \max_{||u||=||v||=1} Cov(\mathbf{Xu}, \mathbf{Yv}). \quad (1)$$

The desired solution for weightings (or often called saliences) $\mathbf{u}$ and $\mathbf{v}$ are the first left and right singular vectors of the cross-block covariance matrix $\mathbf{X}^T\mathbf{Y}$. We here applied the SVD approach to implement the criteria (1) that directly calculates the left and right singular vectors of the covariance matrix $\mathbf{X}^T\mathbf{Y}$. Thus, the main results of this paper further exploit the PLS-SVD algorithm. However, the readers particularly interested in other iterative and kernel-based approaches to PLSC are referred to Supplemental material S1. This also includes the comparison of the underlying orthogonality constraints for PLS-SVD and PLS-NIPALS and the similarity of analysis results of particular PLSC implementations in our NIH dataset.

Application to the NIH study of healthy brain development

Sample

We used a subsample of the NIH MRI study of normal brain development available in the NIH MRI Pediatric MRI Data Repository,

Please cite this article as: Ziegler, G., et al., Partial least squares correlation of multivariate cognitive abilities and local brain structure in children and adolescents, NeuroImage (2013), http://dx.doi.org/10.1016/j.neuroimage.2013.05.088

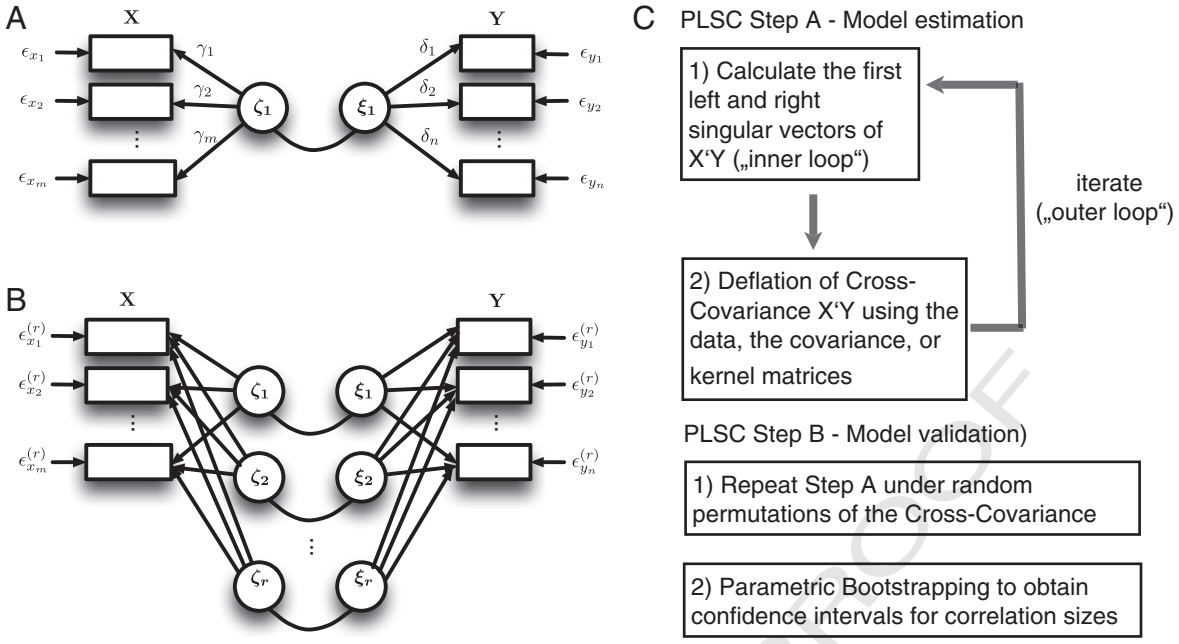

Fig. 1. An overview of the applied PLSC methodology. (A) A single latent variable model is used to explain the covariance of the cognitive variables **X** and brain variables **Y**. The latent variables ζ_1 and ξ_1 reflect the corresponding covariance. The loadings γ and δ are obtained from regression of the latent variables on the data. The resulting residual variances ϵ_{x_i} and ϵ_{y_i} might be correlated and can be analyzed using deflation. (B) The multiple latent variable model after r deflation steps is shown. This results in a sequence of latent variables ζ_i and ξ_i, $i = 1, \ldots, r$ and new regression residuals $\epsilon_{x_i}{}^{(r)}$ and $\epsilon_{y_i}{}^{(r)}$. (C top). (PLSC Step A) Algorithmic structure of the PLSC analysis to analyze covariance structure of data X and Y. The outer loop is used to deflate either the data, the covariance (for PLS-SVD) or the kernel matrices, and the inner loop calculates the corresponding first left and right singular vectors of the covariance $\mathbf{X}^T\mathbf{Y}$. (C bottom) (PLSC Step B) Model selection and validation is performed using permutations testing and bootstrapping respectively. Permutation testing reveals the covariances σ_i under random permutations of rows of X leaving Y unchanged. Parametric bootstrapping is used to assess the stability of the latent variable model parameters by providing confidence intervals.

(https://nihpd.crbs.ucsd.edu). The NIH MRI Pediatric project focuses on brain development in healthy typically developing infants, children and adolescents from a demographically balanced population based sampling (Evans and Group, 2006, for overview). The neuroimaging data was acquired in multiple pediatric centers and included a variety of MR-based sequences and protocols. Moreover, apart from exploring the general course of normal brain development an important part of the project is to reveal the correlation to cognitive and behavioral measures. The screening procedures excluded subjects with a family history of inherited neurological disorders or a lifetime history of Axis I psychiatric disorders, abnormalities during perinatal development, birth complications, physical growth problems, neurological or specific psychiatric disorders. In order to study subjects with normal pediatric development, the behavioral screening excluded subjects with child behavior checklist (CBCL) T-scores < 70, full scale WASI IQ < 70, or Woodcock–Johnson III Achievement Battery subtest scores < 70. A detailed description of the sample acquisition and exclusion criteria can be found in Evans and Group (2006) and here https://nihpd.crbs.-ucsd.edu-/nihpd-/info-/Documents/. We started with a sample from release 4 of the NIH MRI study objective 1 (Almli et al., 2007; Evans and Group, 2006) of the children and adolescents. The full sample included 433 subjects with ages 4.5–18 years. However, due to our focus on cognitive abilities, the sample was reduced to 394 subjects between 6 and 18 years of age with comparable protocols of cognitive testing (see below for details). After checking the completeness of the explicitly rich cognitive test battery, the sample strongly reduced to 307 fully available datasets. We observed variations in raw data slice resolution of the images. These differences strongly influenced the quality of the image preprocessing results. Thus we discarded further 21 scans due to substantial artifacts in segmentation, registration, or nonlinear between-subjects normalization. Finally, the accepted sample consisted of 286 children (151 females, 135 males) with ages 6–18.5 years (M = 11.6, SD = 3.5). The demographic details and descriptive statistics of the analyzed sample are presented in Table 1.

Cognitive ability space

In addition to the MR imaging data, the NIH study of normal brain development included approximately 3 h of neuropsychological assessments of an individual's cognition and behavior using multiple psychometric instruments (Waber et al., 2007). In order to cover a broad spectrum of children's and adolescents' intellectual abilities, we here included a rich set of psychometric measures from the domains of intelligence, processing speed and executive function. All analyzed test scores stem from reliable and validated instruments that were applied using age appropriate test forms. Firstly, we included vocabulary, similarities, matrix reasoning, and block design subtests from the Wechsler Abbreviated Scale of Intelligence (Wechsler, 1999). These measures are typically applied to obtain a brief general intelligence assessment. Additionally, we used measures of processing speed and verbal working memory using the coding task and the digit span task of the Wechsler

Table 1
Demographical description of the sample. Q2

Age group (years)	Subjects	Subjects from site (1/2/3/4/5/6)	Females (%)	FSIQ mean (std)
6–9.5	94	17/16/12/14/12/23	45 (54)	113 (14.3)
9.5–13.5	101	9/24/13/24/10/21	55 (54)	112 (11.1)
13.5–18.5	91	12/14/24/17/10/14	51 (49)	109 (11.2)
Total	286	38/54/49/55/32/58	151 (54)	111 (12.3)

Age groups with number of subjects, gender, as well as mean and standard deviation of general intelligence of the analyzed subsample from the NIH MRI repository. The scanning sites from 1 to 6 are the Children's Hospital Boston, Cincinnati Children's Hospital Medical Center, University of Texas Health Science Center at Houston, University of California in LA, Children's Hospital of Philadelphia, and Washington University in St. Louis, respectively. FSIQ denotes the full scale IQ obtained from Wechsler Abbreviated Scale of Intelligence (WASI).

Please cite this article as: Ziegler, G., et al., Partial least squares correlation of multivariate cognitive abilities and local brain structure in children and adolescents, NeuroImage (2013), http://dx.doi.org/10.1016/j.neuroimage.2013.05.088

Intelligence Scale for Children (WISC-III) and the corresponding score form the Wechsler Adult Intelligence Scale (WAIS-III) for the older adolescents (Wechsler, 1991, 1997). Secondly, Cambridge Neuropsychological Test Battery (CANTAB) is a collection of computerized, non-verbal touchscreen tests for cognitive assessment. Originally developed for diagnosis of cognitive deficits in dementia (Fray and Robbins, 1996), it also became a valid tool for testing children (Luciana, 2003). We included the executive function errors and stages of the Intra-Extra Dimensional Set Shift task (IED) (a computerized version of the Wisconsin Card Sorting test), the Spatial Span (SSP), and Spatial Working Memory (SWM) strategy and responses scores. Thirdly, the Behavior Rating Inventory of Executive Function (BRIEF) was developed to capture the real-world behavioral manifestations of executive dysfunction (Gioia and Isquith, 2004; Gioia et al., 2002a,b, 2010). In contrast to the above performance tests BRIEF uses parents' ratings of their children's everyday executive task performance. We included the metacognition subtests monitor, organization of materials, plan/organize, working memory, initiate as well as the behavioral regulation subtests emotional control, shift, and inhibition. The resulting set of 19 cognitive ability measures (6 WASI/WISC, 5 CANTAB, 8 BRIEF) were raw test scores, *i.e.* usually obtained from sums over items. As the explicit aim of this paper is to estimate the loadings within the cognitive ability space in a single model with the brain data, no separate measurement model was applied. Notably, all BRIEF subtest scores, the CANTAB IED number of errors and both CANTAB SWM scores are originally inverted, *i.e.* higher values originally indicated deficits. In order to simplify interpretation of results in terms of a cognitive manifold of abilities, the sign of all inverted variables was switched. The resulting 19 cognitive measures are positive correlates of intellectual ability and executive function. Before subsequent statistical analysis, an outlier detection procedure was applied, replacing extreme values (*i.e.* more than 3σ) by regression imputation using the highest correlating covariate of the remaining data. The descriptive statistics and the correlation matrix of the recoded cognitive ability parameters are provided in Table 2.

Local brain structure space

A detailed overview of the acquisition protocols of the NIH MRI Pediatric study can be found here (http://pediatricmri.nih.gov/nihpd/info/proto-cols.html). The available sample included data from both primary protocols and fallback protocols with either 1 mm or 3 mm slice thickness, respectively. The preprocessing and analysis steps were done in SPM8 (Wellcome Trust Centre for Neuroimaging, London, UK, http://www.fil.ion.ucl.ac.uk/spm) using the VBM8 toolbox (http://dbm.neu-ro.uni-jena.e/vbm). During preprocessing the images were interpolated to an isotropic resolution of 1.5 mm. The images were (1) corrected for bias-field inhomogeneities, (2) registered using a linear (*i.e.* 12-parameter affine) and a nonlinear diffeomorphic transformation (Ashburner, 2007), and (3) stripped of non-brain tissue in the T1-weighted images. Thereafter, some results from the SPM8 unified segmentation package (Ashburner and Friston, 2005) were used to initialize a VBM8 algorithm that classifies brain tissue in gray matter (GM), white matter (WM), and cerebrospinal fluid (CSF). In order to avoid introducing a systematic bias into the segmentation routine by using the standard adult reference data (Wilke et al., 2003) the Template-O-Matic toolbox (Wilke et al., 2008) was used to generate a sample-specific template. The VBM8 segmentation contains partial volume estimation (PVE) to account for mixed voxels with two tissue types (Tohka et al., 2004). The algorithm uses an adaptive maximum a posteriori (AMAP) approach (Rajapakse et al., 1997) and a subsequent application of a hidden Markov random field model (Cuadra et al., 2005). Within the AMAP estimation the local variations of the parameters (means and variance) are modeled as slowly varying spatial functions. This accounts for intensity inhomogeneities and other local variations. We also included a further quality check using covariance-based inhomogeneity measures of the sample as implemented in the VBM8 toolbox. Thereafter, the resulting gray matter volume images were multiplied voxelwise by the determinants of Jacobian matrices from SPM's nonlinear transformations before subsequent statistical analysis on local volumes. This modulation is done to adjust for local volume changes introduced by the nonlinear normalization. Finally, a smoothing step was performed using a Gaussian kernel of 8 mm full width at half maximum (FWHM). In order to analyze brain regions that have a high probability to contain gray matter tissue, the images were masked by a binary image indicating voxelwise sample mean of gray matter volume (GMV) exceeding absolute threshold of 0.2. All analyses were performed on GMV images obtained using the above steps. After thresholding 315,004 gray matter voxels entered the PLSC modeling. Thus, the voxels served as potentially correlated indicators of structural gray matter network properties in a 315,004 dimensional local brain structure space. The spatial adjacency of voxels was not explicitly used for feature construction but is implicitly reflected by their covariance structure. The brain data will be further denoted with Y.

Effects of confounding variables

Using an observational design to investigate the covariance of brain structure and cognitive abilities, we had to limit the potential influences of covariates. In contrast to a cross-sectional analysis of age-related effects, the analysis of the ability-brain covariation sets a different focus and potentially allows indirect statistical effects between the triplet of age, brain structure, and the cognitive abilities (Salthouse, 2011). A crucial point for neuroanatomic correlates of intelligence is that they might be influenced by confounds, *e.g.* brain size (McDaniel, 2005; Rushton and Ankney, 2009; Taki et al., 2012), global brain parameters (Peelle et al., 2012), gender (Luders et al., 2006, 2009a; Narr et al., 2007; Schmithorst, 2009), and particularly chronological age. This is especially true for studies on early lifespan cognitive abilities, because the size of the expected effects due to individual maturational differences is substantial (Gogtay et al., 2004; Lenroot et al., 2007). In order to focus on individual differences in the local gray matter networks that are independent of age and global brain differences, we applied partialing models to increase the specificity of observed covariations. Global variance removal also decorrelates the local structural features, avoiding the global parameter differences to dominate the regional brain–behavior covariance patterns (see also Supplemental material Fig. S4). This increases the sensitivity to detect local network differences related to cognitive abilities. In addition to obtain the local gray matter segments, VBM8 was used to estimate the absolute tissue volumes in subject's native space. We then corrected the data for cubic age, linear gender, total intracranial volume (using TICV = TGM + TWM + TCSF), and total gray matter volume (TGM) effects using multiple linear regression. Cognitive data **X** and also the brain data Y will denote the corrected data after application of a partialing model including age, age^2, age^3, gender, and TICV, and TGM.

PLSC procedure, model selection and validity

After preprocessing and correcting the NIH sample data for confounds, the above introduced PLS-SVD algorithm was applied to the 19 cognitive tests scores **X** with the VBM gray matter images **Y**. An important issue for appropriate PLSC modeling of the brain–behavior covariance is model selection and statistical inference. Full deflation of the cross-block covariance using the above methods results in a saturated PLSC model, *i.e.* some of the higher-degree latent variables simply fit random covariations of the errors of the blocks. Therefore, nonparametric permutation testing was suggested to assess the significance of the latent variable contribution to the brain–behavior covariance (McIntosh and Lobaugh, 2004). We repeated the PLSC algorithm under 2000 random permutations of the individual cognitive ability data with respect to the brain data. To account for biases due to flipping, reordering and rotations in the resampled data, the observed weightings were transformed to the initial PLSC solution

Please cite this article as: Ziegler, G., et al., Partial least squares correlation of multivariate cognitive abilities and local brain structure in children and adolescents, NeuroImage (2013), http://dx.doi.org/10.1016/j.neuroimage.2013.05.088

Table 2
Cognitive test descriptive statistics and correlation matrix.

	Reasoning	Block	Processing speed	Vocabulary	Similarities	Verbal WM span	SSP span	SWM responses	SWM strategy	IED shift stages	IED shift error	Monitor	Organize material	Plan/ organize	Working-memory	Initiate	Emotional control	Shift	Inhibit
Mean	56.27	55.14	10.67	56.32	56.04	10.78	6.05	−174.59	−32.73	8.20	−22.41	−45.95	−49.24	−16.65	−47.04	−47.97	−45.29	−45.74	−46.61
Std	7.84	9.39	2.90	8.65	9.39	2.64	1.68	26.96	6.55	0.94	13.86	8.84	8.69	3.96	8.26	8.31	8.02	7.78	7.11
Min	30	31	4	28	28	3	2	−233	−45	5	−73	−78	−71	−28	−71	−74	−73	−70	−72
Max	80	80	19	79	80	19	9	−82	−10	9	0	−28	−33	−11	−36	−35	−36	−36	−36
Reasoning	1.00	0.41	0.13	0.42	0.34	0.13	0.22	0.22	0.18	0.11	0.24	0.05	−0.07	0.03	0.07	−0.05	−0.02	−0.01	−0.01
Block	0.41	1.00	0.25	0.31	0.31	0.12	0.31	0.18	0.16	0.19	0.23	0.11	−0.08	0.02	0.08	0.03	0.04	0.07	0.08
Processing speed	0.13	0.25	1.00	0.21	0.23	0.15	0.15	0.09	0.10	0.15	0.25	0.14	0.04	0.19	0.17	0.07	0.09	0.12	0.14
Vocabulary	0.42	0.31	0.21	1.00	0.54	0.29	0.19	0.15	0.14	0.23	0.32	0.06	−0.05	0.09	0.14	0.14	−0.01	0.01	0.08
Similarities	0.34	0.31	0.23	0.54	1.00	0.24	0.14	0.13	0.13	0.16	0.31	0.08	−0.09	0.04	0.08	0.00	−0.08	−0.08	0.12
Verbal WM span	0.13	0.12	0.15	0.29	0.24	1.00	0.18	0.13	0.06	−0.04	0.04	0.09	−0.01	0.06	0.13	0.08	0.00	0.01	0.10
SSP span	0.22	0.31	0.15	0.19	0.14	0.18	1.00	0.08	0.06	0.05	0.14	0.05	−0.02	0.04	0.08	−0.04	0.00	0.00	0.03
SWM responses	0.22	0.18	0.09	0.15	0.13	0.13	0.08	1.00	0.81	−0.14	0.21	0.03	0.02	0.08	0.14	0.02	0.07	0.06	0.10
SWM strategy	0.18	0.16	0.10	0.14	0.13	0.06	0.06	0.81	1.00	−0.10	0.22	0.01	−0.04	0.04	0.07	0.02	0.02	−0.02	0.02
IED shift stages	0.11	0.19	0.15	0.23	0.16	−0.04	0.05	−0.14	−0.10	1.00	0.54	0.07	−0.04	0.06	−0.04	0.05	−0.04	0.08	0.05
IED shift error	0.24	0.23	0.25	0.32	0.31	0.04	0.14	0.21	0.22	0.54	1.00	0.18	−0.03	0.14	0.10	0.12	0.01	0.13	0.20
Monitor	0.05	0.11	0.14	0.06	0.08	0.09	0.05	0.03	0.01	0.07	0.18	1.00	0.48	0.72	0.63	0.61	0.59	0.57	0.65
Organize material	−0.07	−0.08	0.04	−0.05	−0.09	−0.01	−0.02	0.02	−0.04	−0.04	−0.03	0.48	1.00	0.57	0.51	0.50	0.35	0.29	0.36
Plan/organize	0.03	0.02	0.19	0.09	0.04	0.06	0.04	0.08	0.04	0.06	0.14	0.72	0.57	1.00	0.74	0.68	0.51	0.53	0.54
Working-memory	0.07	0.08	0.17	0.14	0.08	0.13	0.08	0.14	0.07	−0.04	0.10	0.63	0.51	0.74	1.00	0.59	0.45	0.49	0.58
Initiate	−0.05	0.03	0.07	0.14	0.00	0.08	−0.04	0.02	0.02	0.05	0.12	0.61	0.50	0.68	0.59	1.00	0.55	0.51	0.50
Emotional control	−0.02	0.04	0.09	−0.01	−0.08	0.00	0.00	0.07	0.02	−0.04	0.01	0.59	0.35	0.51	0.45	0.55	1.00	0.64	0.59
Shift	−0.01	0.07	0.12	0.01	−0.08	0.01	0.00	0.06	−0.02	0.08	0.13	0.57	0.29	0.53	0.49	0.51	0.64	1.00	0.55
Inhibit	−0.01	0.08	0.14	0.08	0.12	0.10	0.03	0.10	0.02	0.05	0.20	0.65	0.36	0.54	0.58	0.50	0.59	0.55	1.00

Mean, standard deviation, and range of the analyzed subtest raw scores (top). Pearson correlation matrix of 19 cognitive ability test scores included in the PLSC analysis (bottom). Reasoning, block, processing speed, vocabulary, similarities, and verbal WM span are subtests from the WASI/WISC battery. SSP span, SWM responses, SWM strategy, IED shift stages, and IED shift error refer to CANTAB's computerized testing subtests of executive functions. Monitor, organize material, plan/organize, working-memory, initiate, emotional control, shift, and inhibit are BRIEF's subtest for executive dysfunction.

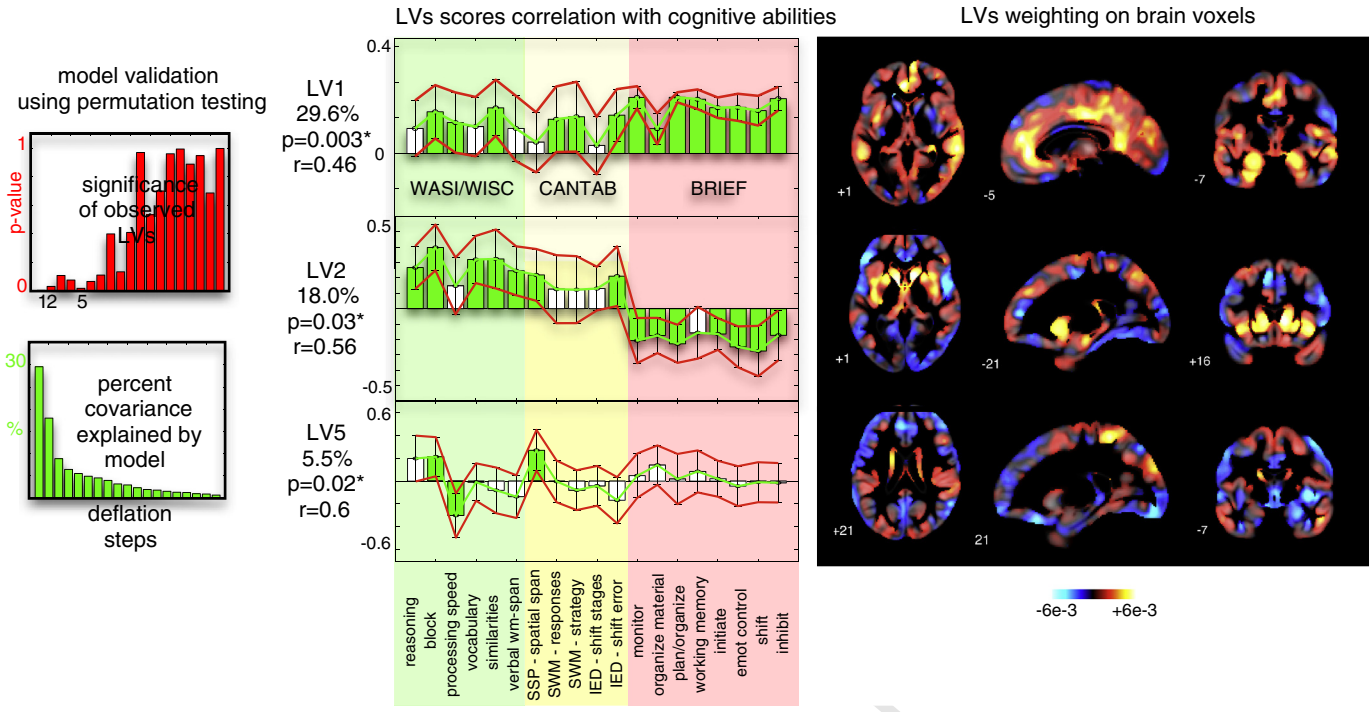

Fig. 2. Partial least squares correlation (PLSC) analysis of 19 cognitive ability scores and local gray matter volume obtained from VBM in 286 children and adolescents, ages 6–18. The brain and cognitive data was first corrected using an appropriate partialing model with age, age^2, age^3, gender, and TICV, TGM then the PLSC estimation was performed using a PLS-SVD approach. Permutation testing revealed the significance of the latent variables. All latent variables with $p < 0.05$ are presented. The cognitive and brain weighting patterns from the PLSC analysis are shown for latent variables 1, 2 and 5. The cognitive ability subtest weightings are standardized in terms of correlations with the corresponding PLSC's brain scores. The red error bars indicate confidence intervals for each subtest's correlations to latent brain scores using 500 parametric bootstrap samples. The observed correlations of latent brain and cognitive scores (*i.e.* $corr(\zeta_i,\xi_i)$) ranged from 0.46 to 0.6.

using procrustes transformations (Milan and Whittaker, 1995). P-values were calculated estimating the probability of observing equal or higher covariances $\sigma_r = Cov(\zeta_\mathbf{r}, \mathbf{xi_r})$ for each of the corresponding latent variables under permutations of the data. Finally, unless stated otherwise the subset of latent variables with $p < 0.05$ was considered to significantly contribute to the covariance. A related issue of PLSC modeling is the validation and confidence in the observed model parameters (Krishnan et al., 2011). PLSC weights and scores imply a covariance of cognitive ability and brain structure which is sensitive to sampling variability and thus requires a cross-validation technique (Efron and Tibshirani, 1994). As suggested by McIntosh et al. (McIntosh and Lobaugh, 2004) we applied parametric bootstrapping to obtain standard errors for the cognitive ability correlations with the latent scores *thbf*ζ_r and ξ_r. We used 500 bootstrap samples by sampling with replacement and further assessed symmetric 95% confidence intervals, *i.e.* $\mu \pm 1.96\sigma$ of the correlation parameter distributions.

Analysis of effects of maturation

In order to realize a group PLSC to analyze age-related differences of the structure–cognition covariance we first reordered rows in the cognitive ability scores and brain data matrices according to 3 age groups with 6–9.5 (n_1=94), 9.5–13.5 (n_2 = 101), and 13.5–18 (n_3 = 91) years, and also obtained: $\mathbf{X}_i$ and $\mathbf{Y}_i$, i = 1, …, 3. The aim was to use age specific cognitive weightings and age independent brain network weightings (which might improve interpretation), we adapted the above maximum covariance criterion (1):

$$\sigma_1 = \max_{||u||=||v||=1} Cov\left(\begin{bmatrix}\mathbf{X}_1\mathbf{u}_1\\ \mathbf{X}_2\mathbf{u}_2\\ \mathbf{X}_3\mathbf{u}_3\end{bmatrix}, \begin{bmatrix}\mathbf{Y}_1\\ \mathbf{Y}_2\\ \mathbf{Y}_3\end{bmatrix}\mathbf{v}\right). \quad (2)$$

This corresponds to searching for first left and right singular vectors of the covariance matrix obtained from row-wise concatenation of age group covariance matrices.

$$\mathbf{C}_{gr} = \begin{bmatrix}\mathbf{X}_1^T\mathbf{Y}_1\\ \mathbf{X}_2^T\mathbf{Y}_2\\ \mathbf{X}_3^T\mathbf{Y}_3\end{bmatrix} = \mathbf{U}\Sigma\mathbf{V}^T = \sum_{r=1}^{R}\sigma_r \begin{bmatrix}\mathbf{u}_{1r}\\ \mathbf{u}_{2r}\\ \mathbf{u}_{3r}\end{bmatrix}\mathbf{v}_r^T$$

This favors the application of the above PLS-SVD algorithm with extended behavioral data vectors. Thus, for our purpose of age-group covariance analysis we applied the PLS-SVD algorithm and model validation procedures to the above covariance matrix C. Separation of the extended cognitive weights, and recalculation of loadings revealed the group specific results.

Results and discussion

Whole group PLSC analysis

We first focused on the PLSC analysis of the whole group of 286 children and adolescents after removing age effects and confounding influences. We directly analyzed the 19 test scores in relation to voxel-based gray matter segments. Fig. 2 shows the obtained PLSC model with latent variable 1 (LV1), ($p = 0.003$, 29.6%), LV2 ($p = 0.03$, 18.0%), and LV5 ($p = 0.02$, 5.5%) showing a significant contribution to the covariance. The dominant LV1 exhibited widespread positive weightings in bilateral medial and superior temporal gyri (including the IPC), frontomedial, anterior and posterior cingulate regions, the precuneus, and early visual areas. In addition, the frontal area 10, the left inferior and middle frontal gyri, the insular cortex, the medial temporal lobe and the left fusiform gyrus showed high weightings. The corresponding cognitive profile revealed more emphasized correlations of

LV1 to BRIEF's executive function scores and minor correlations to intelligence subtests block, similarities, and CANTAB's IED errors. The observed pattern of gray matter volume correlations to multiple cognitive performance scores is in line with observed abilities differences in the large study of Shaw et al. (2006) that revealed positive correlations between IQ and fronto-temporal cortical thickness in the late childhood around age 11. Although the investigated set of tests did not exclusively focus on general intelligence or IQ, LV1 supports findings of early lifespan studies on morphometric correlates of cognitive abilities in the anterior cingulate cortex (Frangou et al., 2004; Karama et al., 2011; Wilke et al., 2003), frontal (Frangou et al., 2004; Karama et al., 2011; Pangelinan et al., 2011; Shaw et al., 2006) and temporo-parietal cortex (Karama et al., 2011; Lange et al., 2010; Shaw et al., 2006). Notably, in contrast to classical paper pencil tests the BRIEF scores represent parents' ratings of children's day to day executive function, organization, planning, working memory skills *etc.* BRIEF's intercorrelations with WASI test scores were found to be low, therefore, WASI and BRIEF represent rather independent aspects of abilities differences (see Table 2).

According to a prevailing theoretical network model for human cognitive ability differences in adults, the Parieto-Frontal Integration Theory (P-FIT), neuronal processing of intelligent behavior is distributed over a wide network of brain regions that are involved in different stages of information processing, *i.e.* recognition, abstraction, problem-solving, and response selection (Jung and Haier, 2007, for review). Although LV1 reflects BRIEF more strongly than WASI, the cortical gray matter regions exhibit a considerable overlap with the proposed set of P-FIT brain regions or modules. We additionally observed a substantial contribution of the hippocampus and the medial temporal lobe gray matter to the dominant LV1. However, the P-FIT theory clearly focuses on higher-level cognitive processes, and thus the existing studies on neuronal substrates of general intelligence measures in the early lifespan (in contrast to studies on elderly subjects) often restrict their analyses to cortical gray matter. A few studies have also suggested the significance of medial temporal lobe regions for childhood cognitive ability in terms of IQ (Deboer et al., 2007; Schumann et al., 2007) and working memory (Østby et al., 2012). The study by Østby et al. (2012) implicated individual differences in children's hippocampal volume as contributing to their long term recall performance after 1 week. We speculate that these effects might be involved in BRIEF's real world planning and metacognition skills found to be highly weighted in LV1.

After projection in the orthogonal subspace from the dominant LV1, the second latent variable LV2 indicated a more mixed pattern, including both positive and negative weightings. In particular, LV2 was found to have positive weightings in subcortical gray matter, especially the caudate nucleus, putamen, and adjacent insular regions, the inferior and superior parietal cortex, precentral area 6, and parts of the superior and middle frontal gyri. However, the remaining cortical regions also showed negative weightings, especially in the left prefrontal cortex and the temporo-parietal regions. Thus, after accounting for the covariance explained by the dominant LV1, those subjects more similar to this mixed pattern tended to have higher WASI scores and slightly lower BRIEF skills in everyday executive function. LV2 exemplifies that interpretation of multivariate analysis across several cognitive domains and brain regions is more complex than for univariate analysis because the effects only make sense using the whole pattern, *i.e.* the cognitive profile and the spatial map. However, LV2's pattern might indicate a different role of striatal and most cortical regional volumes for individual differences in cognitive ability. Notably, the intercorrelations of WASI and CANTAB with BRIEF's test scores are small. Therefore, although both CANTAB and BRIEF focus on executive functions, they represent rather independent sources of variance in our cognitive ability space (see also cognitive tests correlation matrix in Table 2). We suppose LV2's pattern is likely to be driven by two effects that are almost independent in the cognition block: (a) subjects with higher WASI and CANTAB test scores tended to have higher striatal gray matter volume, and (b) subjects with higher BRIEF scores seemed to have more widespread cortical gray matter and slightly less striatal volume. Recent neuroimaging evidence suggests that the basal ganglia, and particularly the dorsal striatum, might be directly involved in higher-level cognitive processes, executive functions and decision making (Balleine et al., 2007; Cools, 2008, 2011; van Schouwenburg et al., 2012). In this line of research van Schouwenburg et al. (2010) used dynamic causal modeling (DCM) (Friston et al., 2003) to demonstrate the functional involvement of striatal circuits in high-level cognitive control. In addition, striatum's association with cognitive ability is supported by structural MRI studies on macroanatomy. Dorsal striatal volume was found to be positively associated with, and additionally predicted, individual differences in children's cognitive control task performance (Chaddock et al., 2010, 2012). Moreover, young adults' initial dorsal striatal volume predicted performance improvement and skill transfer in a video game that explicitly focused on cognitive flexibility (Erickson et al., 2010). These studies support our observation of a positive LV2 weighting for WASI and CANTABs with the basal ganglia volume. The observed pattern of a slightly negative association between local striatum volume and BRIEF's scores is suggested by one recent study by Lange et al. (2010). Finally, we also observed the higher order LV5 ($p < 0.05$). The observed LV5 indicates that higher values of parietal and lateral temporal gray matter networks are associated with individual differences in the block design score, spatial span and processing speed. These regions have been implicated in the P-FIT networks for intelligence differences (Jung and Haier, 2007). However, LV5's contribution to the whole cross-block covariance should be interpreted keeping in mind the much stronger exploratory power of dominant LV1, *i.e.* (5.5% for LV5 *vs.* 29.6% for LV1). Taken together, our PLSC analysis revealed generalizable (spatial and cognitive) patterns and latent variables that contribute to stable individual differences in brain morphology and cognitive ability in the early lifespan. The PLSC models of VBM data revealed latent variable correlations of moderate size 0.46–0.6, which exceeds correlation sizes observed in common univariate models (*e.g.* with IQ Shaw et al., 2006) and supports pattern based analysis in future studies.

Age group PLSC analysis

Individual differences in a cross-sectional observational design might be confounded with age differences. We did account for this possibility by applying appropriate partialing before PLSC modeling, removing the cubic effects of age. Consequently, the above whole group PLSC model approximated a residualized ' average structure–cognition covariance'. However, the developmental processes that cause individual differences in macroanatomy and cognition to covary are likely to undergo changes across developmental stages. Studies using univariate analyses of gray matter networks have provided evidence for maturational changes of the structure–cognition covariance (Karama et al., 2009; Wilke et al., 2003). Thus, a further focus of this work was how the multivariate structure–cognition covariance evolves as a function of age. In order to reintroduce age differences, we extended the above PLSC approach to estimate the covariance separately for ages 6–9.5 years (young), 9.5–13.5 years (middle) and 13.5–18 years (old) in one model (see also Table 1). Firstly, we applied within age group partialing to avoid biased estimates due to the remaining age differences. Secondly, a modified age-group PLSC model was applied. It explicitly allowed group specific cognitive scores and weightings exhibiting the maximal covariance to local gray matter volumes for each group separately. In order to make latent variables and the corresponding gray matter networks comparable, the LV's brain weightings were assumed to be identical across the age groups. Notably, this is not restrictive because each age group can vary with respect to its contribution to a certain LV, *i.e.* which can be strong with high weightings or low with weightings around zero.

Please cite this article as: Ziegler, G., et al., Partial least squares correlation of multivariate cognitive abilities and local brain structure in children and adolescents, NeuroImage (2013), http://dx.doi.org/10.1016/j.neuroimage.2013.05.088

Consequently, if there are group invariant brain patterns we would obtain the age-specific cognitive weightings as intended. Otherwise, the age group variant brain patterns are simply captured by other LVs.

Permutation testing revealed an increased number of contributing LVs compared to the above whole group model (LV1-3 and LV7-10, $p < 0.05$). It indicates that by allowing some age differences to be modeled (or parameterized), more complex models of the multivariate structure–cognition covariance seem to be appropriate. For reasons of space, simplicity, and explained covariance, the first four significant LVs are shown in Fig. 3. Notably, all LVs were found to exhibit group differences, especially comparing the young and middle-aged groups to the adolescents. The inter-correlations of brain weightings from latent variables LV1 ($p < 0.001$, 13%) and LV3 ($p = 0.003$, 7.7%) indicated similarity to the LV1 and LV2 of the whole group PLSC model, respectively. The corresponding gray matter networks were thus consistently observed in our PLSC analyses.

LV1 revealed a late increasing relationship of individual differences in gray matter networks and everyday executive functions as measured by BRIEF. This is in line with the hypothesis of a protracted development of executive functions that continues through childhood into adolescence and early adulthood (Blakemore and Choudhury, 2006; Jurado and Rosselli, 2007, for review). However, the widespread pattern of LV1 does not support an exclusively high relevance of frontal lobe regions for these tasks and also suggests an important role of posterior parts of the brain (Tamnes et al., 2010c, for discussion of this point).

LV2 exhibited a reversal of the estimated covariance between the younger and middle age groups. That means, the pattern of 'more is more' with respect to local gray matter volumes and BRIEF scores switched to a 'more is less' pattern. Similar childhood changes of the direction of the covariance were also observed for measures of general intelligence in a univariate analysis of cortical thickness (see *e.g.* Fig. 1 in Shaw et al., 2006). We speculate that this might be related to the onset of cortical fine-tuning of networks in terms of cellular processes that increase efficiency of information processing, *e.g.* pruning, dendritic changes and myelination. LV3, similar to LV2 in the whole group PLSC model, showed strong positive weightings in the striatum and mixed positive and negative weightings in other cortical networks. The childhood behavioral correlations seemed to 'move' from BRIEF to WASI and CANTAB during early adolescence. As discussed for the whole group PLSC model, this variable might indicate a mixture of effects. Inspecting the results of the age-group model, we additionally observed indications for a developmental change of the role of basal ganglia and cortical volumes in cognitive ability.

Interestingly, the posterior gray matter network of LV7 showed specific association to CANTAB's spatial working memory and set shifting tests (see also Tamnes et al., 2010c). In particular, this latent variable was positively associated with gray matter volume in the precuneus, the posterior cingulate (PCC) and retrosplenial (RSC) cortices, the lingual gyrus, the inferior and superior parietal cortices, the left fusiform and parahippocampal gyri. As recently reviewed by Kravitz et al. (2011), human visuo-spatial processing in the 'dorsal stream' is likely to be driven by three complex subsystems of anatomical and functional connectivity projecting from the parietal cortex to either prefrontal, premotor or medial temporal lobe regions respectively (Margulies et al., 2009). The observed brain pattern emphasizes individual gray matter volume differences in the latter subsystem of

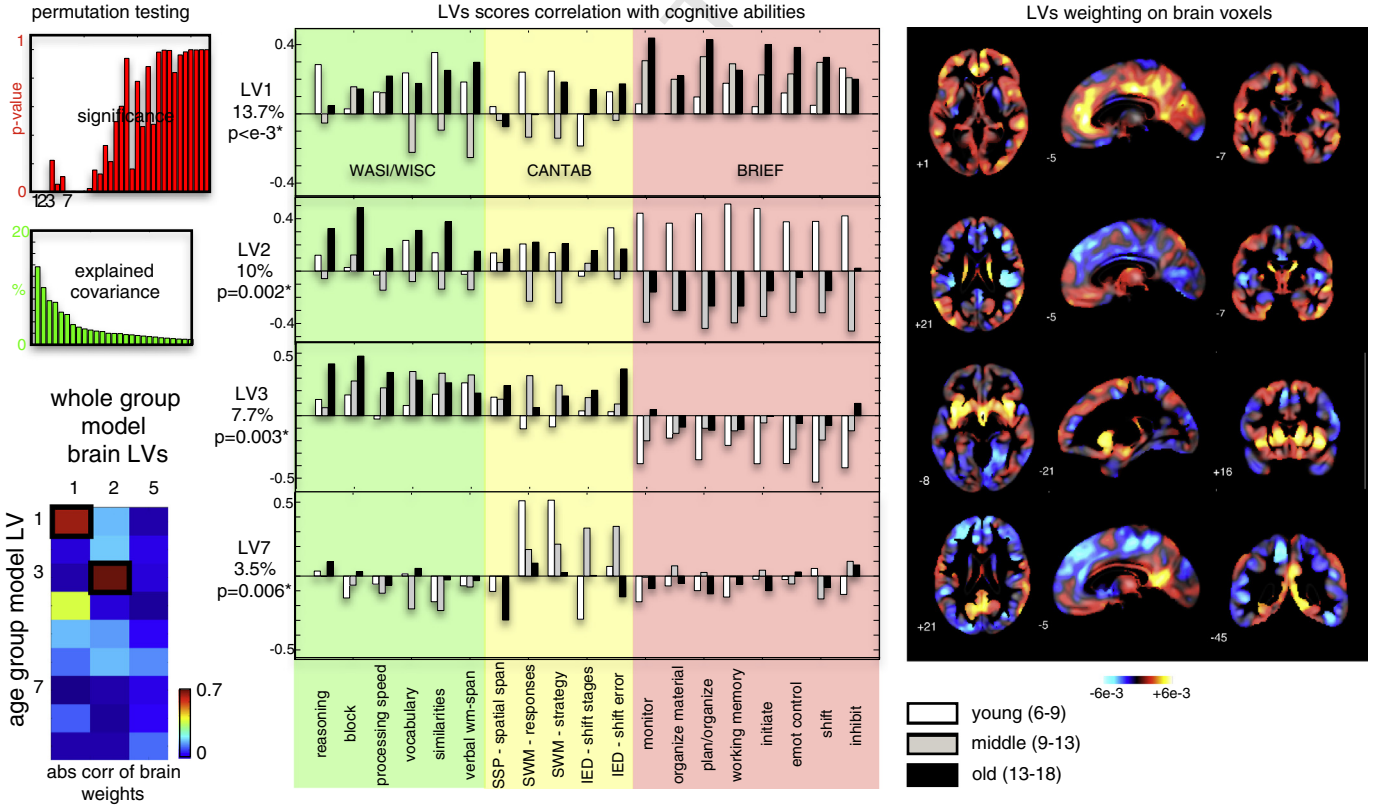

Fig. 3. Analysis of maturation of the structure–cognition covariance in 286 children and adolescents using age groups with 6–9, 9–13.5, and 13.5–18 years respectively. The data was processed using a within age group partialing model with confounders age, age^2, age^3, gender, TICV, and TGM. The PLSC model was used to estimate group specific cognitive weighting profiles (see methods section for details). Permutation testing revealed significance of LVs. Shown are LVs 1, 2, 3 and 7 with $p < 0.05$. The similarity to LVs in the whole group PLSC model was identified using absolute correlations of the brain weighting patterns. Each age group can vary with respect to its contribution to a certain LV, *i.e.* strong with high weightings or low with weightings around zero.

Please cite this article as: Ziegler, G., et al., Partial least squares correlation of multivariate cognitive abilities and local brain structure in children and adolescents, NeuroImage (2013), http://dx.doi.org/10.1016/j.neuroimage.2013.05.088

medial pathways (*via* PCC and RSC) that are suggested to relay and integrate spatial information from the occipito-parietal system to the hippocampal formation and the parahippocampal cortex (Kravitz et al., 2011). The contribution of these regions to SWM performance differences is also supported by human functional MRI studies of navigation (Grön et al., 2000; Maguire et al., 1998), visual motion (Antal et al., 2008), and visual short-term memory (Mitchell and Cusack, 2008; Todd and Marois, 2004). In contrast to the above LVs, the LV7 covariance here exhibits a 'fade out' pattern, with higher covariance in children compared to adolescent subjects. This early childhood covariance to posterior networks would be in line with the anterior posterior gradient of structural maturation (*e.g.* shown for cortical thickness in Shaw, 2008). Occipito-parietal visual systems are found to mature earlier compared to more fronto-temporal networks.

There are limitations of the current study that could be addressed in future work. Firstly, the available cognitive tests WASI/WISC, CANTAB and BRIEF in the NIH data repository have been applied assuming the reliability and validity of the psychometric tools (see also Waber et al., 2007). When using PLSC as an exploratory tool for brain analysis with multiple cognitive scores, there are no assumptions about the measurement model in the age groups. However, we cannot exclude that observed age group differences are also related to inherent limitations of the cognitive assessments tools, *e.g.* variability of sensitivity and validity between age groups. Artifacts from test invariance would be rather likely to occur in single subtests and not influence the whole observed pattern across the 19 scores. This is supported by the inspection of the correlation matrices of the cognitive scores, which indicated no substantial age-related changes (see Supplemental material Table S3). Secondly, the applied PLSC scheme is cross-sectional and uses cubic age models for residualized analysis of individual differences. Therefore, we cannot separate brain–cognition covariance that is due to already existing differences (from earlier maturation periods) and brain–cognition covariance due to ongoing structural changes, *e.g.* pruning in adolescents. Further studies might disentangle these contributions to our findings by using analysis of individual structural trajectories obtained from longitudinal data. Thirdly, the spatial brain features in our PLSC model were restricted to local gray matter segments obtained from VBM. Additionally, efficiency of cognitive processing is expected to require a fast communication between these gray matter regions (Tamnes et al., 2010a,b). It would be promising to also include other modalities, *e.g.* local white matter volumes (WMV) and diffusion tensor imaging (DTI) data. Along with this idea, a recent unsupervised learning method called link independent component analysis (Link ICA) was suggested to jointly analyze individual and age-related differences across MRI modalities (Groves et al., 2011, 2012). The PLSC deflations result in orthogonal latent variables while ICA aims at finding spatially-independent non-Gaussian sources, which might be less restrictive. Finally, analogous to basic factor analytic methods, maximizing the covariance in PLSC comes at the cost of having most cognitive test scores load on all latent variables. Future studies might also focus on appropriate 'non-oblique' rotation techniques within the PLSC framework, which transform the observed pattern of brain–behavior covariance weights into a 'simple structure'.

Conclusion

Here we considered multivariate PLSC models to explore the relationship between cognitive ability patterns and the fine-grained differences in local brain anatomy measured with MRI. We investigated these joint variations in healthy children and adolescents and observed that cognitive patterns explain substantial amounts of structural differences in the maturing brain. The multivariate approach revealed latent variable correlations between morphological patterns and cognitive profiles, suggesting more complex brain–behavior models. Moreover, the findings suggest dynamic changes of the multivariate structure–cognition covariance as a process of brain maturation.

Supplementary data to this article can be found online at http://dx.doi.org/10.1016/j.neuroimage.2013.05.088.

Conflict of interest statement

The authors declare that there are neither actual nor potential conflicts of interest.

Acknowledgments

This work was supported in part by BMBF grants (01EV0709 and 01GW0740). Data used in the preparation of this article were obtained from the NIH Pediatric MRI Data Repository created by the NIH MRI Study of Normal Brain Development. This is a multisite, longitudinal study of typically developing children from ages newborn through young adulthood conducted by the Brain Development Cooperative Group and supported by the National Institute of Child Health and Human Development, the National Institute on Drug Abuse, the National Institute of Mental Health, and the National Institute of Neurological Disorders and Stroke (Contract #s N01-HD02-3343, N01-MH9-0002, and N01-NS-9-2314, -2315, -2316, -2317, -2319 and -2320). A listing of the participating sites and a complete listing of the study investigators can be found at http://www.bic.mni.mcgill.ca/nihpd/info/participa-ting_cen-ters.html. Notably, this manuscript reflects the views of the authors and may not reflect the opinions or views of the NIH.

References

Ackerman, P.L., Beier, M.E., Boyle, M.O., 2005. Working memory and intelligence: the same or different constructs? Psychol. Bull. 131 (1), 30–60.
Almli, C.R., Rivkin, M.J., McKinstry, R.C., Brain Development Cooperative Group, 2007. The NIH MRI study of normal brain development (objective-2): newborns, infants, toddlers, and preschoolers. Neuroimage 35 (1), 308–325.
Antal, A., Baudewig, J., Paulus, W., Dechent, P., 2008. The posterior cingulate cortex and planum temporale/parietal operculum are activated by coherent visual motion. Vis. Neurosci. 25 (1), 17–26.
Ardila, A., Pineda, D., Rosselli, M., 2000. Correlation between intelligence test scores and executive function measures. Arch. Clin. Neuropsychol. 15 (1), 31–36.
Ashburner, J., 2007. A fast diffeomorphic image registration algorithm. Neuroimage 38 (1), 95–113.
Ashburner, J., Friston, K.J., 2005. Unified segmentation. Neuroimage 26 (3), 839–851.
Balleine, B.W., Delgado, M.R., Hikosaka, O., 2007. The role of the dorsal striatum in reward and decision-making. J. Neurosci. 27 (31), 8161–8165.
Barbey, A.K., Colom, R., Grafman, J., 2012. Distributed neural system for emotional intelligence revealed by lesion mapping. Soc. Cogn. Affect. Neurosci. Q6
Bartholomew, D., 2004. Measuring Intelligence: Facts and Fallacies. Cambridge Univ Pr.
Blakemore, S.-J., Choudhury, S., 2006. Development of the adolescent brain: implications for executive function and social cognition. J. Child Psychol. Psychiatry 47 (3–4), 296–312.
Borga, M., Landelius, T., K.H., 1992. A unified approach to PCA, PLS, MLR and CCA. Technical Report, ISY. Q7
Bray, S., Chang, C., Hoeft, F., 2009. Applications of multivariate pattern classification analyses in developmental neuroimaging of healthy and clinical populations. Front. Hum. Neurosci. 3, 32.
Carroll, J., 1993. Human Cognitive Abilities: A Survey of Factor-Analytic Studies. Cambridge University Press.
Chaddock, L., Erickson, K.I., Prakash, R.S., VanPatter, M., Voss, M.W., Pontifex, M.B., Raine, L.B., Hillman, C.H., Kramer, A.F., 2010. Basal ganglia volume is associated with aerobic fitness in preadolescent children. Dev. Neurosci. 32 (3), 249–256.
Chaddock, L., Hillman, C.H., Pontifex, M.B., Johnson, C.R., Raine, L.B., Kramer, A.F., 2012. Childhood aerobic fitness predicts cognitive performance one year later. J. Sports Sci. 30 (5), 421–430.
Chan, R.C.K., Shum, D., Toulopoulou, T., Chen, E.Y.H., 2008. Assessment of executive functions: review of instruments and identification of critical issues. Arch. Clin. Neuropsychol. 23 (2), 201–216.
Colom, R., Jung, R.E., Haier, R.J., 2006. Distributed brain sites for the g-factor of intelligence. Neuroimage 31 (3), 1359–1365.
Colom, R., Jung, R.E., Haier, R.J., 2007. General intelligence and memory span: evidence for a common neuroanatomic framework. Cogn. Neuropsychol. 24 (8), 867–878.
Colom, R., Karama, S., Jung, R.E., Haier, R.J., 2010. Human intelligence and brain networks. Dialogues Clin. Neurosci. 12 (4), 489–501.
Cools, R., 2008. Role of dopamine in the motivational and cognitive control of behavior. Neuroscientist 14 (4), 381–395.
Cools, R., 2011. Dopaminergic control of the striatum for high-level cognition. Curr. Opin. Neurobiol. 21 (3), 402–407.
Cuadra, M.B., Cammoun, L., Butz, T., Cuisenaire, O., Thiran, J.P., 2005. Comparison and validation of tissue modelization and statistical classification methods in T1-weighted MR brain images. IEEE Trans. Med. Imaging 24, 1548–1565.

Please cite this article as: Ziegler, G., et al., Partial least squares correlation of multivariate cognitive abilities and local brain structure in children and adolescents, NeuroImage (2013), http://dx.doi.org/10.1016/j.neuroimage.2013.05.088

Deary, I.J., 2012. Intelligence. Annu. Rev. Psychol. 63, 453–482.
Deary, I.J., Penke, L., Johnson, W., 2010. The neuroscience of human intelligence differences. Nat. Rev. Neurosci. 11 (3), 201–211.
Deboer, T., Wu, Z., Lee, A., Simon, T.J., 2007. Hippocampal volume reduction in children with chromosome 22q11.2 deletion syndrome is associated with cognitive impairment. Behav. Brain Funct. 3, 54.
Dosenbach, N.U.F., Nardos, B., Cohen, A.L., Fair, D.A., Power, J.D., Church, J.A., Nelson, S.M., Wig, G.S., Vogel, A.C., Lessov-Schlaggar, C.N., Barnes, K.A., Dubis, J.W., Feczko, E., Coalson, R.S., Pruett, J.R., Barch, D.M., Petersen, S.E., Schlaggar, B.L., 2010. Prediction of individual brain maturity using fMRI. Science 329 (5997), 1358–1361.
Ebisch, S.J., Perrucci, M.G., Mercuri, P., Romanelli, R., Mantini, D., Romani, G.L., Colom, R., Saggino, A., 2012. Common and unique neuro-functional basis of induction, visualization, and spatial relationships as cognitive components of fluid intelligence. Neuroimage 62 (1), 331–342.
Efron, B., Tibshirani, R.J., 1994. An Introduction to the Bootstrap. Chapman and Hall.
Erickson, K.I., Boot, W.R., Basak, C., Neider, M.B., Prakash, R.S., Voss, M.W., Graybiel, A.M., Simons, D.J., Fabiani, M., Gratton, G., Kramer, A.F., 2010. Striatal volume predicts level of video game skill acquisition. Cereb. Cortex 20 (11), 2522–2530.
Evans, A.C., Group, B.D.C., 2006. The NIH MRI study of normal brain development. Neuroimage 30 (1), 184–202.
Frangou, S., Chitins, X., Williams, S.C.R., 2004. Mapping IQ and gray matter density in healthy young people. Neuroimage 23 (3), 800–805.
Fray, P.J., Robbins, T.W., 1996. CANTAB battery: proposed utility in neurotoxicology. Neurotoxicol. Teratol. 18 (4), 499–504.
Friedman, N.P., Miyake, A., Corley, R.P., Young, S.E., Defries, J.C., Hewitt, J.K., 2006. Not all executive functions are related to intelligence. Psychol. Sci. 17 (2), 172–179.
Friedman, N.P., Miyake, A., Young, S.E., Defries, J.C., Corley, R.P., Hewitt, J.K., 2008. Individual differences in executive functions are almost entirely genetic in origin. J. Exp. Psychol. Gen. 137 (2), 201–225.
Friston, K.J., Harrison, L., Penny, W., 2003. Dynamic causal modelling. Neuroimage 19 (4), 1273–1302.
Geladi, P., 1988. Notes on the history and nature of partial least squares (PLS) modelling. Chemometrics 2 (4), 231–246.
Giedd, J.N., Rapoport, J.L., 2010. Structural MRI of pediatric brain development: what have we learned and where are we going? Neuron 67 (5), 728–734.
Gioia, G.A., Isquith, P.K., 2004. Ecological assessment of executive function in traumatic brain injury. Dev. Neuropsychol. 25 (1–2), 135–158.
Gioia, G.A., Isquith, P.K., Kenworthy, L., Barton, R.M., 2002a. Profiles of everyday executive function in acquired and developmental disorders. Child Neuropsychol. 8 (2), 121–137.
Gioia, G.A., Isquith, P.K., Retzlaff, P.D., Espy, K.A., 2002b. Confirmatory factor analysis of the behavior rating inventory of executive function (brief) in a clinical sample. Child Neuropsychol. 8 (4), 249–257.
Gioia, G.A., Kenworthy, L., Isquith, P.K., 2010. Executive function in the real world: brief lessons from Mark Ylvisaker. J. Head Trauma Rehabil. 25 (6), 433–439.
Gläscher, J., Rudrauf, D., Colom, R., Paul, L.K., Tranel, D., Damasio, H., Adolphs, R., 2010. Distributed neural system for general intelligence revealed by lesion mapping. Proc. Natl. Acad. Sci. U. S. A. 107 (10), 4705–4709.
Gogtay, N., Giedd, J.N., Lusk, L., Hayashi, K.M., Greenstein, D., Vaituzis, A.C., Nugent, T.F., Herman, D.H., Clasen, L.S., Toga, A.W., Rapoport, J.L., Thompson, P.M., 2004. Dynamic mapping of human cortical development during childhood through early adulthood. Proc. Natl. Acad. Sci. U. S. A. 101 (21), 8174–8179.
Grön, G., Wunderlich, A.P., Spitzer, M., Tomczak, R., Riepe, M.W., 2000. Brain activation during human navigation: gender-different neural networks as substrate of performance. Nat. Neurosci. 3 (4), 404–408.
Groves, A.R., Beckmann, C.F., Smith, S.M., Woolrich, M.W., 2011. Linked independent component analysis for multimodal data fusion. Neuroimage 54 (3), 2198–2217.
Groves, A.R., Smith, S.M., Fjell, A.M., Tamnes, C.K., Walhovd, K.B., Douaud, G., Woolrich, M.W., Westlye, L.T., 2012. Benefits of multi-modal fusion analysis on a large-scale dataset: life-span patterns of inter-subject variability in cortical morphometry and white matter microstructure. Neuroimage 63 (1), 365–380.
Haier, R.J., Jung, R.E., Yeo, R.A., Head, K., Alkire, M.T., 2004. Structural brain variation and general intelligence. Neuroimage 23 (1), 425–433.
Hoeft, F., McCandliss, B.D., Black, J.M., Gantman, A., Zakerani, N., Hulme, C., Lyytinen, H., Whitfield-Gabrieli, S., Glover, G.H., Reiss, A.L., Gabrieli, J.D.E., 2011. Neural systems predicting long-term outcome in dyslexia. Proc. Natl. Acad. Sci. U. S. A. 108 (1), 361–366.
Hoeskuldsson, A., 1988. PLS regression methods. Chemometrics 2 (3), 211–228.
Jensen, A., 1998. The G Factor: The Science of Mental Ability. Praeger, Westport, CT.
Jung, R.E., Haier, R.J., 2007. The pareto-frontal integration theory (p-fit) of intelligence: converging neuroimaging evidence. Behav. Brain Sci. 30 (2), 135–154 (discussion 154–87).
Jurado, M.B., Rosselli, M., 2007. The elusive nature of executive functions: a review of our current understanding. Neuropsychol. Rev. 17 (3), 213–233.
Kanai, R., Rees, G., 2011. The structural basis of inter-individual differences in human behaviour and cognition. Nat. Rev. Neurosci. 12 (4), 231–242.
Karama, S., Ad-Dab'bagh, Y., Haier, R., Deary, I.J., 2009. Erratum to "positive association between cognitive ability and cortical thickness in a representative us sample of healthy 6 to 18 year-olds". Intelligence. http://dx.doi.org/10.1016/j.intell.2008.09.006.
Karama, S., Colom, R., Johnson, W., Deary, I.J., Haier, R., Waber, D.P., Lepage, C., Ganjavi, H., Jung, R., Evans, A.C., Group, B.D.C., 2011. Cortical thickness correlates of specific cognitive performance accounted for by the general factor of intelligence in healthy children aged 6 to 18. Neuroimage 55 (4), 1443–1453.
Koutsouleris, N., Gaser, C., Bottlender, R., Davatzikos, C., Decker, P., Jäger, M., Schmitt, G., Reiser, M., Möller, H.-J., Meisenzahl, E.M., 2010. Use of neuroanatomical pattern regression to predict the structural brain dynamics of vulnerability and transition to psychosis. Schizophr. Res. 123 (2–3), 175–187.
Kravitz, D.J., Saleem, K.S., Baker, C.I., Mishkin, M., 2011. A new neural framework for visuospatial processing. Nat. Rev. Neurosci. 12 (4), 217–230.
Krishnan, A., Williams, L.J., McIntosh, A.R., Abdi, H., 2011. Partial least squares (PLS) methods for neuroimaging: a tutorial and review. Neuroimage 56 (2), 455–475.
Lange, N., Froimowitz, M.P., Bigler, E.D., Lainhart, J.E., Group, B.D.C., 2010. Associations between IQ, total and regional brain volumes, and demography in a large normative sample of healthy children and adolescents. Dev. Neuropsychol. 35 (3), 296–317.
Lenroot, R.K., Giedd, J.N., 2006. Brain development in children and adolescents: insights from anatomical magnetic resonance imaging. Neurosci. Biobehav. Rev. 30 (6), 718–729.
Lenroot, R.K., Gogtay, N., Greenstein, D.K., Wells, E.M., Wallace, G.L., Clasen, L.S., Blumenthal, J.D., Lerch, J.P., Zijdenbos, A.P., Evans, A.C., Thompson, P.M., Giedd, J.N., 2007. Sexual dimorphism of brain developmental trajectories during childhood and adolescence. Neuroimage 36 (4), 1065–1073.
Lerch, J.P., Worsley, K.J., Shaw, W.P., Greenstein, D.K., Lenroot, R.K., Giedd, J.N., Evans, A.C., 2006. Mapping anatomical correlations across cerebral cortex (MACACC) using cortical thickness from MRI. Neuroimage 31 (3), 993–1003.
Luciana, M., 2003. Practitioner review: computerized assessment of neuropsychological function in children: clinical and research applications of the Cambridge neuropsychological testing automated battery (CANTAB). J. Child Psychol. Psychiatry 44 (5), 649–663.
Luders, E., Narr, K.L., Thompson, P.M., Rex, D.E., Woods, R.P., Deluca, H., Jancke, L., Toga, A.W., 2006. Gender effects on cortical thickness and the influence of scaling. Hum. Brain Mapp. 27 (4), 314–324.
Luders, E., Narr, K.L., Bilder, R.M., Thompson, P.M., Szeszko, P.R., Hamilton, L., Toga, A.W., 2007. Positive correlations between corpus callosum thickness and intelligence. Neuroimage 37 (4), 1457–1464.
Luders, E., Narr, K.L., Bilder, R.M., Szeszko, P.R., Gurbani, M.N., Hamilton, L., Toga, A.W., Gaser, C., 2008. Mapping the relationship between cortical convolution and intelligence: effects of gender. Cereb. Cortex 18 (9), 2019–2026.
Luders, E., Gaser, C., Narr, K.L., Toga, A.W., 2009a. Why sex matters: brain size independent differences in gray matter distributions between men and women. J. Neurosci. 29 (45), 14265–14270.
Luders, E., Narr, K.L., Thompson, P.M., Toga, A.W., 2009b. Neuroanatomical correlates of intelligence. Intelligence 37 (2), 156–163.
Luders, E., Thompson, P.M., Narr, K.L., Zamanyan, A., Chou, Y.-Y., Gutman, B., Dinov, I.D., Toga, A.W., 2011. The link between callosal thickness and intelligence in healthy children and adolescents. Neuroimage 54 (3), 1823–1830.
Maguire, E.A., Burgess, N., Donnett, J.G., Frackowiak, R.S., Frith, C.D., O'Keefe, J., 1998. Knowing where and getting there: a human navigation network. Science 280 (5365), 921–924.
Margulies, D.S., Vincent, J.L., Kelly, C., Lohmann, G., Uddin, L.Q., Biswal, B.B., Villringer, A., Castellanos, F.X., Milham, M.P., Petrides, M., 2009. Precuneus shares intrinsic functional architecture in humans and monkeys. Proc. Natl. Acad. Sci. U. S. A. 106 (47), 20069–20074.
McDaniel, M.A., 2005. Big-brained people are smarter: a meta-analysis of the relationship between in vivo brain volume and intelligence. Intelligence 33, 337–346.
McIntosh, A.R., Lobaugh, N.J., 2004. Partial least squares analysis of neuroimaging data: applications and advances. Neuroimage 23 (Suppl. 1), S250–S263.
McIntosh, A.R., Bookstein, F.L., Haxby, J.V., Grady, C.L., 1996. Spatial pattern analysis of functional brain images using partial least squares. Neuroimage 3 (3 Pt 1), 143–157.
McIntosh, A.R., Chau, W.K., Protzner, A.B., 2004. Spatiotemporal analysis of event-related fMRI data using partial least squares. Neuroimage 23 (2), 764–775.
Mietchen, D., Gaser, C., 2009. Computational morphometry for detecting changes in brain structure due to development, aging, learning, disease and evolution. Front. Neuroinform. 3, 25.
Milan, L., Whittaker, J., 1995. Applications of the parameteric bootstrap to models that incorporate a singular value decomposition. J. R. Stat. Soc.: Ser. C: Appl. Stat. 44 (1), 31–49.
Misaki, M., Wallace, G.L., Dankner, N., Martin, A., Bandettini, P.A., 2012. Characteristic cortical thickness patterns in adolescents with autism spectrum disorders: interactions with age and intellectual ability revealed by canonical correlation analysis. Neuroimage 60 (3), 1890–1901.
Mitchell, D.J., Cusack, R., 2008. Flexible, capacity-limited activity of posterior parietal cortex in perceptual as well as visual short-term memory tasks. Cereb. Cortex 18 (8), 1788–1798.
Monti, M.M., 2011. Statistical analysis of fMRI time-series: a critical review of the GLM approach. Front. Hum. Neurosci. 5, 28.
Narr, K.L., Woods, R.P., Thompson, P.M., Szeszko, P., Robinson, D., Dimtcheva, T., Gurbani, M., Toga, A.W., Bilder, R.M., 2007. Relationships between IQ and regional cortical gray matter thickness in healthy adults. Cereb. Cortex 17 (9), 2163–2171.
Ostby, Y., Tamnes, C.K., Fjell, A.M., Westlye, L.T., Due-Tønnessen, P., Walhovd, K.B., 2009. Heterogeneity in subcortical brain development: a structural magnetic resonance imaging study of brain maturation from 8 to 30 years. J. Neurosci. 29 (38), 11772–11782.
Østby, Y., Tamnes, C.K., Fjell, A.M., Walhovd, K.B., 2011. Morphometry and connectivity of the fronto-parietal verbal working memory network in development. Neuropsychologia 49 (14), 3854–3862.
Østby, Y., Tamnes, C.K., Fjell, A.M., Walhovd, K.B., 2012. Dissociating memory processes in the developing brain: the role of hippocampal volume and cortical thickness in recall after minutes versus days. Cereb. Cortex 22 (2), 381–390.
Pangelinan, M.M., Zhang, G., VanMeter, J.W., Clark, J.E., Hatfield, B.D., Haufler, A.J., 2011. Beyond age and gender: relationships between cortical and subcortical brain volume and cognitive-motor abilities in school-age children. Neuroimage 54 (4), 3093–3100.

Please cite this article as: Ziegler, G., et al., Partial least squares correlation of multivariate cognitive abilities and local brain structure in children and adolescents, NeuroImage (2013), http://dx.doi.org/10.1016/j.neuroimage.2013.05.088

Peelle, J.E., Cusack, R., Henson, R.N.A., 2012. Adjusting for global effects in voxel-based morphometry: gray matter decline in normal aging. Neuroimage 60 (2), 1503–1516.
Porter, J.N., Collins, P.F., Muetzel, R.L., Lim, K.O., Luciana, M., 2011. Associations between cortical thickness and verbal fluency in childhood, adolescence, and young adulthood. Neuroimage 55 (4), 1865–1877.
Rajapakse, J.C., Giedd, J.N., Rapoport, J.L., 1997. Statistical approach to segmentation of single-channel cerebral MR images. IEEE Trans. Med. Imaging 16 (2), 176–186.
Ramsden, S., Richardson, F.M., Josse, G., Thomas, M.S.C., Ellis, C., Shakeshaft, C., Seghier, M.L., Price, C.J., 2011. Verbal and non-verbal intelligence changes in the teenage brain. Nature 479 (7371), 113–116.
Rushton, J.P., Ankney, C.D., 2009. Whole brain size and general mental ability: a review. Int. J. Neurosci. 119 (5), 691–731.
Salthouse, T.A., 2011. Cognitive correlates of cross-sectional differences and longitudinal changes in trail making performance. J. Clin. Exp. Neuropsychol. 33 (2), 242–248.
Salthouse, T.A., Atkinson, T.M., Berish, D.E., 2003. Executive functioning as a potential mediator of age-related cognitive decline in normal adults. J. Exp. Psychol. Gen. 132 (4), 566–594.
Schmithorst, V.J., 2009. Developmental sex differences in the relation of neuroanatomical connectivity to intelligence. Intelligence 37 (2), 164–173.
Schumann, C.M., Hamstra, J., Goodlin-Jones, B.L., Kwon, H., Reiss, A.L., Amaral, D.G., 2007. Hippocampal size positively correlates with verbal IQ in male children. Hippocampus 17 (6), 486–493.
Shaw, L.M., 2008. Penn biomarker core of the Alzheimer's disease neuroimaging initiative. Neurosignals 16 (1), 19–23.
Shaw, P., Greenstein, D., Lerch, J.P., Clasen, L., Lenroot, R., Gogtay, N., Evans, A.C., Rapoport, J., Giedd, J.N., 2006. Intellectual ability and cortical development in children and adolescents. Nature 440 (7084), 676–679.
Shawe-Taylor, J., Cristianini, N., 2004. Kernel Methods for Pattern Analysis. Cambridge University Press.
Shelton, J.T., Elliott, E.M., Hill, B.D., Calamia, M.R., Gouvier, W.D., 2009. A comparison of laboratory and clinical working memory tests and their prediction of fluid intelligence. Intelligence 37 (3), 283.
Sowell, E.R., Thompson, P.M., Toga, A.W., 2004. Mapping changes in the human cortex throughout the span of life. Neuroscientist 10 (4), 372–392.
Spearman, C., 1904. General intelligence objectively determined and measured. Am. J. Psychol. 15, 201–293.
Taki, Y., Hashizume, H., Sassa, Y., Takeuchi, H., Asano, M., Asano, K., Kotozaki, Y., Nouchi, R., Wu, K., Fukuda, H., Kawashima, R., 2012. Correlation among body height, intelligence, and brain gray matter volume in healthy children. Neuroimage 59 (2), 1023–1027.
Tamnes, C.K., Ostby, Y., Fjell, A.M., Westlye, L.T., Due-Tønnessen, P., Walhovd, K.B., 2010a. Brain maturation in adolescence and young adulthood: regional age-related changes in cortical thickness and white matter volume and microstructure. Cereb. Cortex 20 (3), 534–548.
Tamnes, C.K., Østby, Y., Walhovd, K.B., Westlye, L.T., Due-Tønnessen, P., Fjell, A.M., 2010b. Intellectual abilities and white matter microstructure in development: a diffusion tensor imaging study. Hum. Brain Mapp. 31 (10), 1609–1625.
Tamnes, C.K., Østby, Y., Walhovd, K.B., Westlye, L.T., Due-Tønnessen, P., Fjell, A.M., 2010c. Neuroanatomical correlates of executive functions in children and adolescents: a magnetic resonance imaging (MRI) study of cortical thickness. Neuropsychologia 48 (9), 2496–2508.
Tamnes, C.K., Fjell, A.M., Ostby, Y., Westlye, L.T., Due-Tønnessen, P., Bjørnerud, A., Walhovd, K.B., 2011. The brain dynamics of intellectual development: Waxing and waning white and gray matter. Neuropsychologia 49 (13), 3605–3611.
Tau, G.Z., Peterson, B.S., 2010. Normal development of brain circuits. Neuropsychopharmacology 35 (1), 147–168.
Todd, J.J., Marois, R., 2004. Capacity limit of visual short-term memory in human posterior parietal cortex. Nature 428 (6984), 751–754.
Toga, A.W., Thompson, P.M., 2003. Temporal dynamics of brain anatomy. Annu. Rev. Biomed. Eng. 5, 119–145.
Tohka, J., Zijdenbos, A., Evans, A., 2004. Fast and robust parameter estimation for statistical partial volume models in brain MRI. Neuroimage 23 (1), 84–97.
van Schouwenburg, M.R., den Ouden, H.E.M., Cools, R., 2010. The human basal ganglia modulate frontal-posterior connectivity during attention shifting. J. Neurosci. 30 (29), 9910–9918.
van Schouwenburg, M.R., O'Shea, J., Mars, R.B., Rushworth, M.F.S., Cools, R., 2012. Controlling human striatal cognitive function *via* the frontal cortex. J. Neurosci. 32 (16), 5631–5637.
Waber, D.P., De Moor, C., Forbes, P.W., Almli, C.R., Botteron, K.N., Leonard, G., Milovan, D., Paus, T., Rumsey, J., Brain Development Cooperative Group, 2007. The NIH MRI study of normal brain development: performance of a population based sample of healthy children aged 6 to 18 years on a neuropsychological battery. J. Int. Neuropsychol. Soc. 13 (5), 729–746.
Wechsler, D., 1991. Wechsler Intelligence Scale for Children, 3rd edition. Psychological Corporation, New York.
Wechsler, D., 1997. Wechsler Adult Intelligence Scale. The Psychological Corporation, San Antonio, TX.
Wechsler, D., 1999. Wechsler Abbreviated Scale of Intelligence. Psychological Corporation, New York.
Wegelin, J.A., 2000. A survey of partial least squares (PLS) methods, with emphasis on the two-block case. Technical Report.Department of Statistics, University of Washington.
Wilke, M., Sohn, J.-H., Byars, A.W., Holland, S.K., 2003. Bright spots: correlations of gray matter volume with IQ in a normal pediatric population. Neuroimage 20 (1), 202–215.
Wilke, M., Holland, S.K., Altaye, M., Gaser, C., 2008. Template-o-matic: a toolbox for creating customized pediatric templates. Neuroimage 41 (3), 903–913.
Wold, H., 1975. Path models with latent variables: the NIPALS approach. In: Blalock, H.M. (Ed.), Quantitative Sociology: International Perspectives on Mathematical and Statistical Modeling, pp. 307–357 (Academic).
Wold, H., 1982. Soft modeling: the basic design and some extensions. In: Jöreskog, K.G. (Ed.), Systems under indirect observation: causality, structure, prediction, Part II, vol. 2. North Holland Publishing Company, Amsterdam, pp. 1–54.

Please cite this article as: Ziegler, G., et al., Partial least squares correlation of multivariate cognitive abilities and local brain structure in children and adolescents, NeuroImage (2013), http://dx.doi.org/10.1016/j.neuroimage.2013.05.088